Title:

Elastically and Plastically Foldable Electro-Thermal Micro-Origami for Controllable and Rapid Shape Morphing

*Yi Zhu, Mayur Birla, Kenn R. Oldham, and Evgueni T. Filipov**

Yi Zhu, Prof. Evgueni T. Filipov

University of Michigan, Department of Civil and Environmental Engineering

2350 Hayward Street, Ann Arbor, MI, USA, 48109.

E-mail: filipov@umich.edu

Mayur Birla, Prof. Kenn Oldham
University of Michigan, Department of Mechanical Engineering

2350 Hayward Street, Ann Arbor, MI, USA, 48109.

Keywords: micro-origami, programmable metamaterial, rapid folding, micro-electro-mechanical systems, electro-thermal actuators

Abstract:

Integrating origami principles within traditional micro-fabrication methods can produce shape morphing micro-scale metamaterials and 3D systems with complex geometries and programmable mechanical properties. However, available micro-origami systems usually have slow folding speeds, provide few active degrees-of-freedom, rely on environmental stimuli for actuation, and allow for either elastic or plastic folding but not both. This work introduces an integrated fabrication-design-actuation methodology of an electro-thermal micro-origami system that addresses the abovementioned challenges. Controllable and localized joule heating from electro-thermal actuator arrays enables rapid, large-angle, and reversible elastic folding, while overheating can achieve plastic folding to reprogram the static 3D geometry. Because the proposed micro-origami do not rely on an environmental stimulus for actuation, they can function in different atmospheric environments and perform controllable multi-degrees-of-freedom shape morphing, allowing them to achieve complex motions and advanced functions. Combining the elastic and plastic folding enables these micro-origami to first fold plastically into a desired geometry and then fold elastically to perform a function or for enhanced shape morphing. The proposed origami systems are suitable for creating medical devices, metamaterials, and micro-robots, where rapid folding and enhanced control are desired.

1. Introduction

Origami, the art of folding, provides a viable method to transform planar 2D surfaces into functional 3D structures and systems including foldable robots [1,2], deployable space structures[3], reconfigurable architectural structures[4], metamaterials[5-7] and more. Within the field of 2D photolithography-based microfabrication processes, origami offers transformative advancements in creating 3D systems and assemblies[8,9], making it possible to fold practical micro-scale systems such as bio-medical devices[10-12], drug delivery micro-containers[13], and shape morphing materials[14]. Pragmatic solutions to fold origami type structures at small scales include using active or responsive material systems such as hydrogels[15-17], bimetallic morphs[18,19], passive hinges with magnetic panels[20-24], and several others[25-28].

Despite the advancements in designing and building micro-origami inspired systems, the examples presented above have one or more limitations. Many of these shape morphing processes require carefully planned variation in environmental stimuli such as changing temperatures[14,15], applying chemical exposures[12], or applying external magnetic fields[20-24] , so these systems have difficulty to function in less controlled atmospheric environments outside of a laboratory. Another major limitation of this reliance on an environmental stimulus is that these shape morphing systems usually have only one active degree-of-freedom[15] (a shape morphing path with either folding motion or unfolding motion), and thus they cannot control multiple active degrees-of-freedom for shape morphing, or to complete complex tasks. Furthermore, these systems usually require a relatively long time to achieve large folding, either because of the inherently slow shape morphing mechanisms[26] or because it takes time to change the environmental properties such as heating up the water surrounding the system[14,15]. Finally, most of the previous micro-origami systems can either achieve folding elastically or plastically but not both, which limits the functionality and geometric programmability that can be achieved by these systems.

Although micro-scale origami is a relatively young field of research, there has been related work on creating actuators for micro-electro-mechanical systems (MEMS) that provides helpful insight on how to implement active systems at small scales. Piezoelectric material-based actuators, electro-thermal actuators, and electro-static actuators are capable of achieving out-of-plane motions [29-34], and the electro-thermal actuators show potential for generating relatively large folding angles [35]. However, most of these currently available electro-thermal actuator designs are not capable of folding beyond 90 degrees from the initial flat state, which limits their usage for application in micro-origami systems where complex shapes with large folding are desired. Moreover, it is not yet clear how to integrate these actuators organically into origami patterns such that accurate shape morphing and proper functions are realized.

To address the abovementioned problems, we propose a new integrated fabrication-design-actuation method to embed a new electro-thermal actuator design within micro-origami systems. The elastic folding of this micro-origami is achieved by locally controlled joule heating of origami creases which fold due to differential thermal expansion between gold and polymer layers. This elastic folding is controllable, rapid, and reversible, giving the micro-origami high performance shape morphing with multiple active degrees-of-freedom (number of circuits that can be heated separately) to realize versatile and complex functionalities. In addition to the elastic folding, the systems can achieve plastic folding to reprogram the *zero current rest angle* of creases (fold angle at which no current is applied). This plastic folding is achieved by overheating the crease to create a visco-elasto-plastic material response while applying an external load on the crease. The proposed micro-origami systems are easy to fabricate with a three-mask process because we use a thin film of gold to simultaneously serve as the controlling circuit, the passive layer, and the electro-thermal heater. The enhanced performance and versatility of these systems can be used to create controllable and rapid shape morphing metamaterials and 3D systems for applications in micro-robots, microelectromechanical systems, metamaterials, transducers, and more.

This work is organized in the following order. First, we introduce the design method and fabrication process of the proposed electro-thermal micro-origami. Next, we use experiments to demonstrate folding capability of these micro-origami, showing that the proposed system can achieve elastic folding with large angles and rapid speeds at varying atmospheric temperatures, and can also achieve plastic folding to reprogram their zero current rest angles. Then, two origami 3D gripper systems are introduced to demonstrate the enhanced control and multiple active degrees-of-freedom of the proposed systems. Finally, we introduce two methods to fabricate complex origami patterns, one by combining active folds and passive folds and the other by combining the elastic folding and the plastic folding. We envision that the proposed micro-origami system can greatly expand the possible motions and functions realizable by functional small-scale shape morphing systems.

2. Results and Discussions

2.1. Customizable Design and Easy Fabrication

This section introduces the design methodology and the fabrication method for the proposed electro-thermal micro-origami and demonstrates the versatility and simplicity of the process. **Figure.1** (a) shows the fabrication flow chart of the proposed micro-origami. First, a thin film of SU-8

(0.8 µm) is deposited and patterned on top of a silicon wafer; Next, a thin film of gold (0.2 µm, with 0.01 µm adhesive Cr film below) is deposited with E-beam evaporation and patterned by wet etch; A thick film of SU-8 (20 µm) is next deposited and patterned by photolithography to create the panels, and finally, the origami system is released with Xenon Difluoride etching. This fabrication method is versatile and can build different origami simultaneously. Tailored design of the origami pattern is used to ensure the desired folding behavior and to create metamaterials and 3D systems with different geometries and functionalities. (see Figure 1. (b))

Figure 1. (c) shows the design of the bi-layer electro-thermal actuator used to drive the micro-origami. We choose gold and SU-8 for their relatively large difference in thermal expansion coefficients (TEC)[36]. This relatively large difference in the TEC (α_{Au} = 14 ppm K^{-1}, $\alpha_{SU\text{-}8}$ =52 ppm K^{-1}) allows the actuators to achieve large folding angles because the thin SU-8 layer expands more than the gold when the region is heated. When the input current is low (less than about 6.5 mA), such actuator arrays can generate rapid and large folding elastically and reversibly. However, when the actuator arrays are heated towards the glass transition temperature of SU-8 (Tg=210°C) with currents reaching about 8 mA, the SU-8 films will experience visco-elasto-plastic material responses and can deform plastically under applied forces. Therefore, by controlling the input current, we can make the same actuator arrays to deform both elastically and plastically based on our needs. This capability to control and induce plastic deformation is discussed in Section 2.2 and offers unprecedented novelty in active reprogramming of the 3D folded shape.

In this micro-origami design, the gold layer serves multiple functions, which include: (1) Strengthening the surface of the thin film SU-8 to prevent upwards bending triggered by residual stress (see SI Figure S2); (2) Heating up the actuators locally; (3) Acting as an electronic circuit to control folding creases separately; (4) Serving as the passive layer for the large difference in TEC. With this high level of function integration, the process is greatly simplified and only needs three masks. The proposed fabrication cannot create actuators that actively bend downwards because putting gold film under the thin film SU-8 triggers unwanted residual stress profile (see SI Figure S2). However, as will be demonstrated later, it is possible to bypass this problem by creating origami designs that use actuators only for upward folding creases while leaving downward folding creases as elastic springs. By arranging these actuators into arrays and connecting them with thick SU-8 panels (see Figure 1. (d)), a *single-crease origami* is made. This is the basic building block of more complicated origami patterns. Figure 1. (e) shows the detailed dimensions of the benchmark single-crease origami tested in this article. Although we only fabricate and test designs in the range of 1mm for a panel, the complete system can be scaled up and down with the same principle of design to build 3D shape morphing systems at different scales.

2.2. Folding Performance of Creases

The folding performance of individual origami creases controls the global performance of the origami shape morphing systems. Thus, it is important to ensure that these creases within the origami systems can fold efficiently, swiftly, and powerfully. In this section, the single-crease origami system is tested in detail to highlight its four most attractive capabilities: (1) to achieve large folding rotations reversibly (forming an acute interior angle with greater than 90° folding from the initial orientation); (2) to function in atmospheric environments with different temperatures; (3) to fold rapidly; (4) to have the *zero current rest angle* reprogrammed. The first three abilities highlight the good performance of the elastic folding, while the last ability enables the plastic folding to reprogram the shape of the micro-origami. These four capabilities ensure a satisfying shape morphing performance of the proposed micro-origami system for building active and functional metamaterials and 3D systems at small scales.

These single-crease origami can be elastically folded by applying a current through the heaters and the behavior of these single-crease origami is summarized in **Figure 2**. Figure 2. (a) shows the relationship between the folding angle and current for single-crease origami with different actuator lengths, and Figure 2. (b) shows the measured current-voltage relationships. Longer actuators can give higher folding angles at the same current level but require higher voltage input. It takes about 3.0 V of voltage and 20 mW of power to fold these single-crease origami to a right angle. These inputs are reasonable considering the ability to achieve large and rapid folding. Because the panels in these structures are thick and heavy (20 times thicker than the actuator), these single-crease origami tend to rest at negative folding angles under the influence of gravity. A threshold current is required to overcome gravity and to lift the panel off from the silicon wafer. However, this threshold current is difficult to determine because the negative folding region cannot be visually observed. Thus, dotted lines are used in Figures 2. (a) and (d) to indicate this effect. Section S4 provides further analysis on the threshold effects due to the presence of gravity.

The single-crease origami systems can fold elastically in common atmospheric temperatures (Figure 2. (c), Video S1). Results for actuation at 1°C to 49°C show that although the systems are affected by the environmental temperature, it is possible to offset the influence by changing the current and the voltage input (Figure 2. (d), and experimental details in Figure S4 of SI). We select this temperature range because it represents common temperature range of outdoor atmospheric environments. The systems can function around and below freezing temperatures, however the zero current rest angle is negative, which is restricted by the wafer below and cannot be observed (Figure 2. (d)).

This single-crease system can also achieve rapid elastic folding up to and slightly beyond resonance. We demonstrate this behavior using sine wave sweeping tests (from 1 Hz to 200 Hz) with three different input voltage setups (see Figure 2. (e) and (f)). The folding motion is mostly quasi-static when the frequency is low. However, as the input frequency increases, the response becomes dynamic: the motion range decreases gradually until 20 to 40 Hz and then increases to a peak at the resonance frequency. We recorded the single-crease origami oscillating with a folding range of about 65° at resonance of about 77 Hz when voltage is cycled from 1.35V to 1.65V, which gives an average speed of about 10000° sec^{-1}. A simple analytical model is used to estimate the resonance frequency (SI section S4) with no material softening due to elevated temperature. At a higher frequency of 150 Hz, the sample only oscillates locally with small motion, because the actuators cannot heat and cool fast enough at higher frequencies. The system demonstrated a longer fundamental period as we increase the AC voltage amplitude or increase the DC voltage offset. This period elongation occurs because the actuator is working at higher temperature when the voltage is higher, which in turn causes the material to become softer. Video S1 shows the loading behavior of these single-crease systems with step voltage input (on/off with no ramp). Higher order dynamic vibration excited by the step loading dies out rapidly, indicating that the systems have relatively high damping. The rapid folding ability of the proposed system is far beyond what is offered by most existing micro-origami systems that require more than several seconds to fold[14--19]. The high folding speed of the proposed micro-origami offers an unprecedented ability to achieve rapid and responsive shape morphing systems at the micro-scale.

Another major advantage of the proposed micro-origami is that the creases can be controlled to fold both elastically and plastically by changing the input current. This ability to modify the crease behavior greatly enhances the versatility and functionality of the system and allows for controlled programming and reprogramming of the folded shape. **Figure 3.** (a) shows a schematic illustration of how we can achieve this plastic folding by overheating the thin film SU-8 to temperatures where it exhibits visco-elasto-plastic material response, and while in this state, applying forces to reprogram the zero current rest angle of creases. Figure 3. (b) demonstrates a proof-of-concept experiment we conducted to twice reprogram a single-crease origami with 200 µm long actuator beams. At the beginning, the zero current rest angle of this single-crease origami is zero degrees. The crease folds and unfolds reversibly, when applying and removing the 2.4 V of input voltage, and no obvious plastic deformation is observed for multiple cycles of loading. However, when 3.0 V are applied across the circuit, the crease folds beyond 90° and the SU-8 polymer starts to experience a visco-elasto-plastic material behavior. At this state, the influence of gravity further deforms the crease (it acts as an external load), and the zero current rest angle is reprogrammed. After removing the applied current, this single-crease origami has about ten degrees of plastic deformation, and its reversible motion from 0V to 2.4 V is also offset by the same amount (Figure 3. (b)). Next, we can recover the original zero current rest angle by directly pressing down on the panel and reapplying 3.0 V to overheat the crease again. The amount of plastic deformation in the crease is affected by the magnitude of the force and the duration of overheating as briefly shown with control tests in Video S2.

Figure 3. (c) to (e) show the measured hysteretic folding curves of the single-crease micro-origami, where two loading cycles are applied to systems with 200 µm and 400 µm long actuator beams. We first sequentially applied the loading cycle A, cycle B, and cycle A on to the single-crease origami with 200 µm beams and record its folding angle (Figure 3. (e)). During the first cycle A loading, no plastic

folding is observed because the voltage is low and the unloading curve falls directly on top of the loading curve. However, plastic folding is observed during the cycle B loading, because the applied voltage is high and it causes the SU-8 material to deform visco-elasto-plastically. At the end of the loading cycle B, the zero current rest angle is changed to 10 degrees from the perfectly flat state. When a second loading cycle A is applied, we again do not observed plastic folding. The loading and unloading curves coincide but are offset by the new zero current rest angle. We next applied the loading cycle B onto a single-crease origami with 400 μm actuator beams, and the loading curve shows that no plastic folding or hysteresis is developed during the process. This is because longer actuators have higher resistance and thus generate lower temperatures when the same voltage is applied.

Because this plastic folding technique does not require continuous energy input after the reprogramming, it provides an energy efficient solution for creating 3D systems that do not need to recover their original flat configurations. Moreover, we showed that we can trigger this plastic folding by creating actuators that are shorter and by applying extra current to overheat the crease region. When this reprogramming method is used to permanently change the shape of these micro-origami, passive folds that act like elastic springs can be integrated into the system to generate this external force, which will be demonstrated in section 2.4.

2.3. Controllable Multi-Degree-of-Freedom Shape Morphing for Complex Functionalities

One beneficial feature of the proposed micro-origami is that it can have multiple active degrees-of-freedom and thus can achieve shape morphing motions with a higher level of versatility. In this section, we highlight these abilities by demonstrating two designs of 3D origami grippers that achieve advanced shape morphing motions and sophisticated functions. We select the large-displacement micro-gripper as our target because it is difficult to create this type of mechanisms with traditional micro-fabrication process at smaller scales [36,37]. With traditional MEMS based methods, out-of-plane motions for gripping can be achieved with different actuator systems [29-34]. However, existing systems usually have folding angles of less than 90°, and have been difficult to integrate into origami designs with more complex motions and functions. Separate attempts have created 3D assembly with large folding angles using tradition MEMS processes, but these systems usually require manual assembly with probe stations [38-40] or through an applied magnetic field [20-24]. We show that with the proposed method, we can self-assemble the gripper and achieve a large gripping motion using the same base design. The two micro-origami grippers can both achieve millimeter range gripping motion but have different characteristics: one preserves the ability to reconfigure back to flat while the other maintains the folded configuration with locking mechanisms. These grippers are useful tools to realize the self-assembly and "fabrication on a chip" concepts for micro-system packaging and other applications.

Figure 4. shows an origami gripper that can undergo controllable multi-degree-of-freedom shape morphing to perform large-range gripping and is robust enough to survive a wet environment where it is sprinkled with water. This micro-origami has two side panels for 3D assembly and two gripper panels acting as gripping arms. First, we apply a voltage across the assembly circuit to fold the gripper into its functional state; next, we apply a voltage across the function circuit to grip; finally, we can release the voltage in both circuits after usage and the origami returns to its original flat position. The origami is next subjected to a wet environment where it was sprinkled with water (Figure 4. (c), Video S3). The cooling effects of water evaporation dramatically changes the local

thermal environment and leads to unreliable folding actuation at points where water was sprayed. However, as the water dries, the origami recovers its ability to fold and grip. As demonstrated in this example, the multiple active degrees-of-freedom enables the gripper to achieve “assemble and function” shape morphing that is beyond simple “fold and unfold” motions.

The second gripper design can lock into a functional 3D state, where it can remain without additional input of current (**Figure 5**. (a)). The origami pattern is designed such that the two pins on the base panel can slide into the two holes on the top panel to create an interlocked 3D geometry (Figure 5. (b)). Because shape morphing of these active origami systems do not rely on changing environmental stimulus, we can achieve a controllable multi-degree-of-freedom shape morphing process needed for the 3D locking assembly, where the two 20 μm thick pins can be aligned precisely with the two 60 μm wide holes. To achieve this locking motion, the actuator arrays in the base panel are required to fold to a large angle (almost 180°), which is difficult to achieve with standard MEMS actuators, such as those in [29-34]. After locking, the system remains assembled when the current in the circuits is removed. A third circuit is then used to actuate the gripping motion for the system functionality. This active system can be more energy efficient for multiple uses, because after assembly no input current or external stimulus is needed to hold the 3D geometry. Moreover, the interlocking effects make the 3D assembly more mechanically robust against various effects that can affect the functionality of micro-scale systems, such as changes in the temperature of the atmospheric environment.

2.4. Towards Complex Origami

In this section, we introduce two techniques to create complex origami systems: one by combining active folds and passive folds, and the other by combining the elastic folding and the plastic folding. Together, the two techniques open up new potentials to create complex origami systems for functional shape morphing and reprogrammable 3D systems at smaller scales.

We first show how we fold origami systems with both mountain and valley folds by using a combination of active and passive folds. To that end, we had to overcome an inherent limitation of the fabrication approach where, only active upward bending of creases is currently possible due to residual stress in the layers (see SI Figure S2). Instead, we use the active folds to generate the upward folding and let those creases that need to fold downward to remain passive and behave like elastic rotational springs. If the pattern is designed to have one degree-of-freedom kinematics, accurate folding can potentially be achieved by only actuating the upward folding creases. The first example is a single Miura-ori unit made up of three active folding creases that bend upwards and one passive crease that deforms like an elastic rotational spring (**Figure 6**. (a) to (c)). The second example is a Miura-ori system with three units that all fold together when actuated (Figure 6. (d) to (f)). Micro-origami structures like these provide a basic building block for micro-actuators or metamaterials[41,42]. The Miura-ori pattern is well known to have one degree-of-freedom kinematics needed for this actuation approach, however origami simulation methods such as the rigid folding algorithm[43,44] can be used to determine if other origami patterns also have one degree-of-freedom kinematics. For more complicated patterns, kinematic analysis alone may not be sufficient to determine if the system can be folded accurately and the placement of actuators will play a significant role [45]. For these more complicated systems, bar and hinge models[46-48] that consider the mechanical properties of an origami can be used to study if the system can fold accurately. As demonstrated in SI Video S5, these micro-origami can alter between unfolded and folded 3D shape swiftly. This rapid responsive ability is superior to many existing systems and allows the proposed micro-origami systems to be used for various applications in robotics and metamaterials, where fast folding is needed.

We next show that by combining the elastic folding and the plastic folding, we can create programmable 3D micro-origami with functions that were not realizable previously. For example, although origami cranes have been folded as smaller scales[15], those systems are not capable of achieving functions such as flapping the wings after having the cranes are folded. In this section an origami crane pattern that can fold and subsequently flap its wings is shown (**Figure 7**. and SI video S5). The plastic folding is used to reprogram the origami shape into a static 3D crane geometry and the elastic folding is subsequently used to flap the wings of this crane. We first apply a current across the folding circuit, to overheat the creases and to develop plastic folding using the forces generated by gravity and the passive folds that tend to revert the pattern back to a flat state (Figure 7. (b)). When we release the applied current, the plastic folding occurs in the reverse direction, and the crane pattern reaches a static folded configuration. After the crane is successfully folded, we can apply current through the wing circuit to elastically flap the wings as shown on Figure 7. (c). With the multiple active degrees-of-freedom provided with the proposed system, the micro-origami can first fold permanently to a desired 3D geometry with one set of plastic folds and then achieve functions with another set of elastic folds. The combination of elastic, plastic, and passive folds allows us to create high performance shape morphing origami systems at smaller scales that were not achievable previously. In practice, designers can use longer actuators to achieve elastic folding at lower functioning temperature or use shorter actuators to achieve higher crease temperature for plastic folding.

3. Conclusion

In this work, a new fabrication-design-actuation methodology for electro-thermal micro-origami systems is introduced and tested in detail. The fabrication of the system is simple and only requires a three masks process, because we integrate multiple functions into a single gold layer. Unlike most existing origami systems, the proposed electro-thermal micro-origami can fold without relying on an environmental stimulus, which allows these micro-origami to achieve rapid and large elastic folding in common atmospheric environments with temperatures ranging from 1°C to 49°C. The proposed origami systems can have the folded state of creases (zero current rest angle of creases) to be reprogrammed by overheating, which provides a method to generate permanently and plastically folded 3D geometries. Experiments show that in addition to having relatively good folding performance, and the folding creases of the proposed micro-origami have reasonable power consumption and require low voltage input. Moreover, because these micro-origami systems do not need environmental stimulus for actuation, they can have multiple active degrees-of-freedom and thus can achieve shape morphing with complex motion paths and a higher level of functional versatility. For example, we present a micro-origami gripper that can align locking pins to locking holes to assemble a mechanically robust interlocked structure that can subsequently perform a large displacement gripping motion. Finally, we introduce two methods to create complex origami systems from unidirectional electro-thermal actuators. The first method combines active and passive folds to create origami patterns with both valley (upward) and mountain (downward) folding directions. Two Miura-ori patterns demonstrate the rapid shape morphing between folded and flat states achieved with the proposed system. The second method uses plastic folding to reprogram the 3D shape of the micro-origami then uses elastic folding to achieve functional motions. An origami crane pattern is presented to demonstrate this method. The crane can first permanently changes its 3D geometry using the plastically folded creases and then flaps its wings with another set of creases that folds elastically.

We believe future research can enhance the capabilities of the proposed systems and overcome limitations presented in the current work. New active polymers can be used to improve the efficiency, folding ability, and control of the residual stress to achieve simultaneous upward and downward actuation. The micro-origami systems can also be integrated with batteries and on-board sensors to create fully autonomous functional 3D micro-systems. The work presented in this paper can serve as a basis for creating shape morphing metamaterials and 3D structures using functional, controllable, and rapidly foldable origami for applications in different atmospheric environments. The integrated fabrication, design, and actuation methodologies provide a customizable framework for future work in micro-scale functional origami systems.

4. Experimental Section

Materials: The SU-8 2000.5 and SU-8 2010 photoresist used in the proposed process are purchased from MicroChem. The gold etchant GE-8111 and chrome etchant 1020 are purchased from Transense. Material properties for these photoresists are obtained from the data sheet produced by the company.

Fabrication process: First, a thin film of SU-8 2000.5 (0.8 µm) is deposited on top of the bare silicon wafer by spin coating. The film is patterned by standard photolithography process and developed using the SU-8 developer. An overnight hard bake at 70 °C is used to further cross-link the polymer. Next, we deposit 0.01 µm of chrome (solely for adhesion) and 0.2 µm of gold on top of the substrate using e-beam evaporation and pattern the two metal layers by wet etch. After patterning the gold layer, we deposit and pattern the SU-8 2010 (20 µm thick) to build the origami panels. Finally, the fabricated micro-origami are released by etching away the silicon substrate with the XeF_2.

Supporting Information

Supporting Information is available from the Wiley Online Library or from the author.

Acknowledgements

The authors acknowledge the support from all staff members from Lurie Nanofabrication Facility, especially K. Beach and P. Herrera-Fierro for their helpful advice and training. The first author would like to acknowledge College of Engineering Dean's Fellowship and College of Engineering Challenge Fellowship from College of Engineering, University of Michigan. The authors appreciate the thoughtful advices from both reviewers, which have improved the quality of this paper. The authors also acknowledge support from DARPA Grant D18AP00071. The paper reflects the views and position of the authors, and not necessarily those of the funding entities.

Received: ((will be filled in by the editorial staff))
Revised: ((will be filled in by the editorial staff))
Published online: ((will be filled in by the editorial staff))

Reference

[1] B. An, S. Miyashita, A. Ong, M. T. Tolley, M. L. Demaine, E. D. Demaine, R. J. Wood, D. Rus, *IEEE Transactions on Robotics* **2018**, 34, 1409-1424.

[2] S. Felton, M. Tolley, E. Demaine, D. Rus, R. Wood, *Science* **2014**, 345, 644-646.

[3] R. J. Lang, S. Magleby, L. Howell, *J. Mech. Robot.* **2016**, 8(3), 031005.

[4] E. T. Filipov, T. Tachi, G. H. Paulino, *Proc. Natl. Acad. Sci. USA,* **2015**, 40, 12321-12326.

[5] M. Schenk, S. D. Guest, *Proc. Natl. Acad. Sci. USA,* **2013**, 110, 3276-3281.

[6] H. Fang, S.-C. A. Chu, Y. Xia, K.-W. Wang, *Adv. Mater.* **2018**, 30(15), 1706311.

[7] S. Kamrava, D. Mousanezhad, H. Ebrahimi, R. Ghosh, A. Vaziri, *Sci. Rep.* **2017**, 7, 46046.

[8] T. G. Leong, A. M. Zarafshar, D. H. Gracias, *Small* **2010**, 6, 792-806.

[9] J. Rogers, Y. Huang, O. G. Schmidt, D. H. Gracias, *MRS Bull.* **2016**, 41(2), 123-129.

[10] E. W. H. Jager, O. Inganas, I. Lundstrom, *Science* **2000**, 288, 2335-2338.

[11] J. C. Breger, C. Yoon, R. Xiao, H. R. Kwag, M. O. Wang, J. P. Fisher, T. D. Nguyen, D. H. Gracias, *ACS Appl. Mater. Interfaces* **2015**, 7, 3398-3405.

[12] T. G. Leong, C. L. Randall, B. R. Benson, N. Bassik, G. M. Stern, D. H. Gracias, *Proc. Natl. Acad. Sci. USA,* **2009**, 106, 703-708.

[13] T. G. Leong, C. L. Randall, B. R. Benson, A. M. Zarafshar, D. H. Gracias, *Lab on a Chip*, **2008**, 8, 1621-1624.

[14] J.-H. Kang, H. Kim, C. D. Santangelo, R. C. Hayward, *Adv. Mater.* **2019**, 31, 0193006.

[15] J.-H. Na, A. A. Evans, J. Bae, M. C. Chiappelli, C. D. Santangelo, R. J. Lang, T. C. Hull, R. C. Hayward, *Adv. Mater.* **2015**, 27, 79-85.

[16] J. L. Silverberg, J.-H. Na, A. A. Evans, B. Liu, T. C. Hull, C. D. Santangelo, R. J. Lang, R. C. Hayward, I. Cohen, *Nat. Mater.* **2015**, 14, 389-393.

[17] C. Yoon, R. Xiao, J. Park, J. Cha, T. D. Nguyen, D. H. Gracias, *Smart Mater. Struct.* **2014**, 23, 094008.

[18] J. S. Randhawa, M. D. Keung, P. Tyagi, D. H. Gracias, *Adv. Mater.* **2010**, 22, 407-410.

[19] N. Bassik, G. M. Stern, D. H. Gracias, *Appl. Phys. Lett.* **2009**, 95, 091901.

[20] N. S. Shaar, G. Barbastathis, C. Livermore, *J. Microelectromech. S.* **2015**, 24, 1043-1051.

[21] J. Kim, S. E. Chung, S.-E. Choi, H. Lee, J. Kim, S. Kwon, *Nat. Mater.* **2011**, 10, 747-752.

[22] E. Iwase, I. Shimoyama, *J. Microelectromech. S.*, **2005**, 14(6) 1265-1271.

[23] Y. W. Yi, C. Liu, *J. Microelectromech. S.*, **1999**, 8 (1) 10-17.

[24] J. Zou, J. Chen, C. Liu, J. E. Schutt-Aine, *J. Microelectromech. S.*, **2001**, 10 (2) 302-309.

[25] R. R. Syms, E. M. Yeatman, V. M. Bright, G. M. Whitesides, *J. Microelectromech. S.*, **2003**, 12 (4) 387-417.

[26] Y. Liu, J. K. Boyles, J. Genzer, M. D. Dickey, *Soft Mater.* **2012**, 8(6), 1764-1769.

[27] H. Fu, K. Nan, W. Bai, W. Huang, K. Bai, L. Lu, C. Zhou, Y. Liu, F. Liu, J. Wang, M. Han, Z. Yan, H. Luan, Y. Zhang, Y. Zhang, J. Zhao, X. Cheng, M. Li, J. W. Lee, Y. Liu, D. Fang, X. Li, Y. Huang, Y. Zhang, J. A. Rogers*, Nat. Mater.* **2018**, 17, 268-276.

[28] X. Ning, X. Yu, H. Wang, R. Sun, R. E. Corman, H. Li, C. M. Lee, Y. Xue, A. Chempakasseril, Y. Yao, Z. Zhang, H. Luan, Z. Wang, W. Xia, X. Feng, R. H. Ewoldt, Y. Huang, Y. Zhang, J. A. Rogers, *Sci. Adv.* **2018**, 4, eaat8313.

[29] K. Suzuki, I. Shimoyama, H. Miura, *J. Microelectromech. S.* **1994**, 3(1), 4-9.

[30] M. Ataka, A. Omodaka, N. Takeshima, H. Fujita, *J. Microelectromech. S.* **1993**, 2(4), 146-150.

[31] J. W. Suh, R. B. Darling, K. F. Bohringer, B. R. Donald, H. Baltes, G. T. Kovacs. *J. Microelectromech. S.* **1999**, 8(4), 483-496.

[32] Y. Suzuki, *Jpn. J. Appl. Phys.*, **1994**, 33(4R) 2107.

[33] C.-H. Rhee, J. S. Pulskamp, R. G. Polcawich, K. R. Oldham, *J. Microelectromech. S.* **2012**, 21(6), 1492-1503.

[34] J. Choi, M. Shin, R. Q. Rudy, C. Kao, J. S. Pulskamp, R. G. Polcawich, K. R. Oldham, *Int. J. Robot. Appl.* **2017**, 1, 180-194.

[35] A. Potekhina, C. Wang, *Actuators*, **2019**, 8(4), 69.

[36] N. Chronis, L. P. Lee, *J. Microelectromech. S.* **2005**, 14, 857-863.

[37] J. Choi, M. Shin, R. Q. Rudy, C. Kao, J. S. Pulskamp, R. G. Polcawich, K. R. Oldham, *Int. J. Intell. Robot. Appl.* **2017**, 1, 180-194.

[38] R. Yeh. E. J. J. Kruglick, K. S. J. Pister *J. Microelectromech. S.* **1996**, 5(1), 10-17.

[39] P. B. Chu, P.R. Nelson, M. L. Tachiki, K. S. Pister, *Sensor. Actuat. A-Phys.,* **1996**, 52(1-3), 216-220.

[40] A. Arevalo, D. Conchouso, D. Castro, M. Diaz, I. G. Foulds, *Micro Nano Lett.*, **2015**, 10(10), 545-549.

[41] H. Fang, S. Li, K. W. Wang, *P. Roy. Soc. A-Math Phy.* **2016**, 472, 20160682.

[42] S. Kamrava, D. Mousanezhad, S. M. Felton, A. Vaziri, *Adv. Mater. Technol.* **2018**, 3, 1870012.

[43] T. Tachi, **2009**, *Origami4* (ed. RJ Lang), 165-174. Natick, MA: A. K. Peters.

[44] T. Tachi*, J. IASS* **2009**, 50, 173-179.

[45] M. Stern, M. B. Pinson, A. Murugan, *Phys. Rev. X*, **2017**, 7, 041070

[46] K. Liu, G. H. Paulino, *P. Roy. Soc. A-Math Phy.* **2017**, 473, 20170348.

[47] Y. Zhu and E. T. Filipov*, J. Mech. Robot.* **2020**, 12, 021110.

[48] Y. Zhu and E. Filipov, *P. Roy. Soc. A-Math Phy.* **2019**, 475, 20190366.

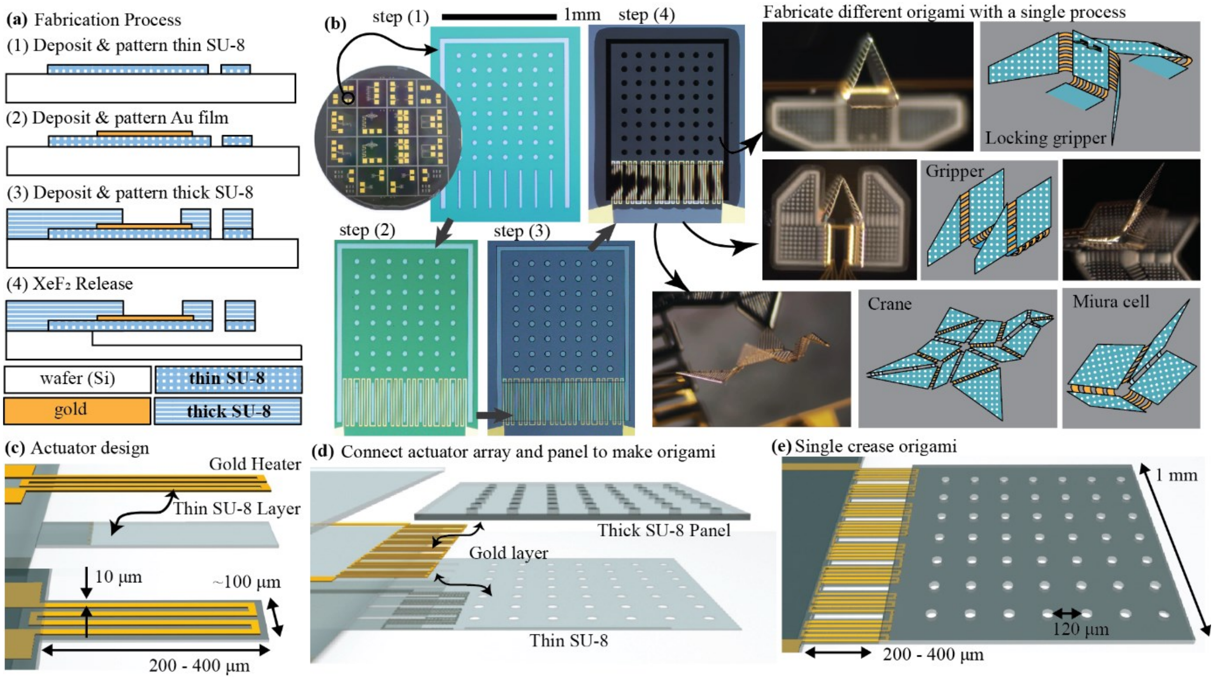

Figure 1. Design and fabrication of the electro-thermal micro-origami systems. (a) Fabrication flow chart; (b) This fabrication method can simultaneously fabricate various micro-origami with different geometries and functions on the same wafer; (c) Design of the electro-thermal actuators; (d) The basic single-crease origami system is made by grouping an array of actuator beams and connecting them to a thick SU-8 panel; (e) Dimensions of a basic single-crease micro-origami system.

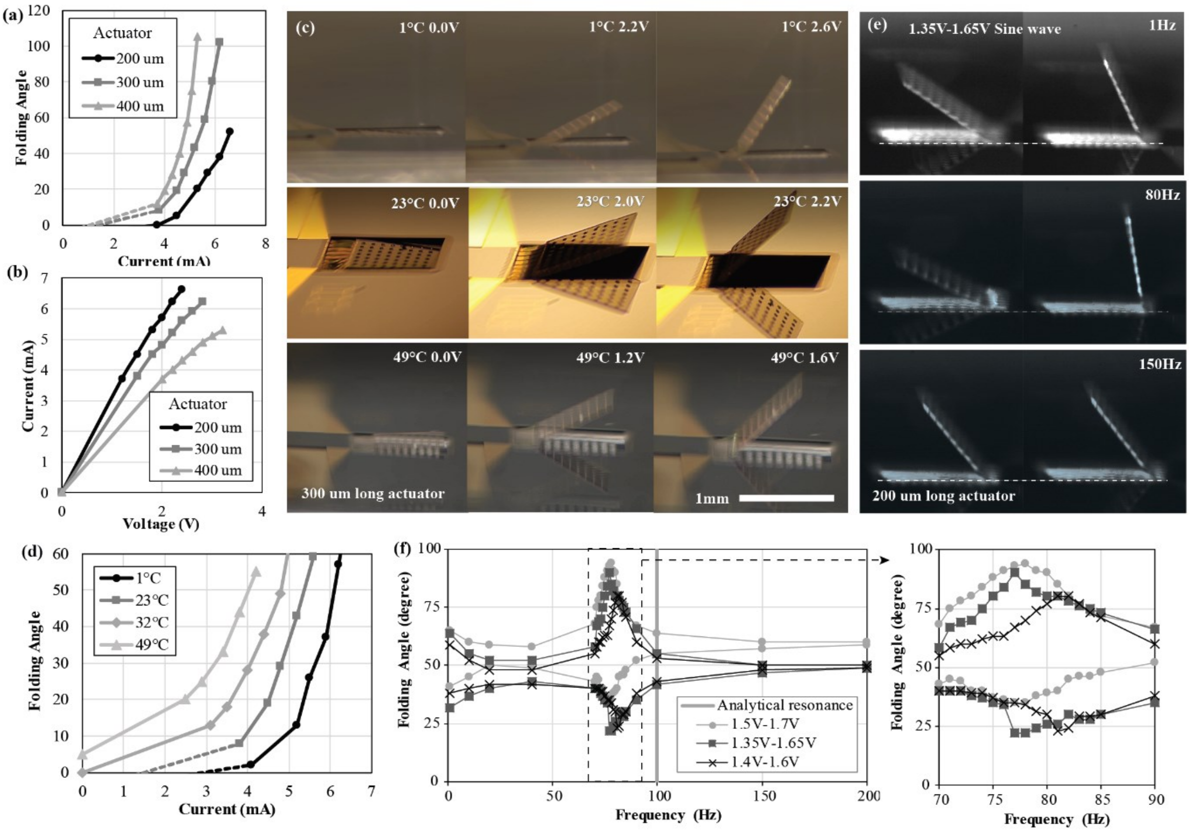

Figure 2. Elastic folding performance of a single-crease origami system. (a) The folding angle with respect to the current for single-crease origami with different actuator beam lengths. A threshold current is required to overcome gravity induced negative folding. However, because this negative folding cannot be observed, approximate dotted lines are used; (b) Measured voltage-current relationship for single-crease origami with different actuator beam lengths; (c) Folded shapes of a single-crease origami with 300 µm long actuators at different atmospheric temperatures; (d) Folding angle with respect to applied current at different temperatures; (e) Dynamic sweeping tests of a micro-origami with 200 µm long actuator; (f) The maximum fold angle (top lines) and minimum fold angle (bottom lines) with respect to frequency of input. A larger AC amplitude or DC offset prolong the fundamental period of single-crease origami. Video S1 shows highlights of the single-crease origami tests.

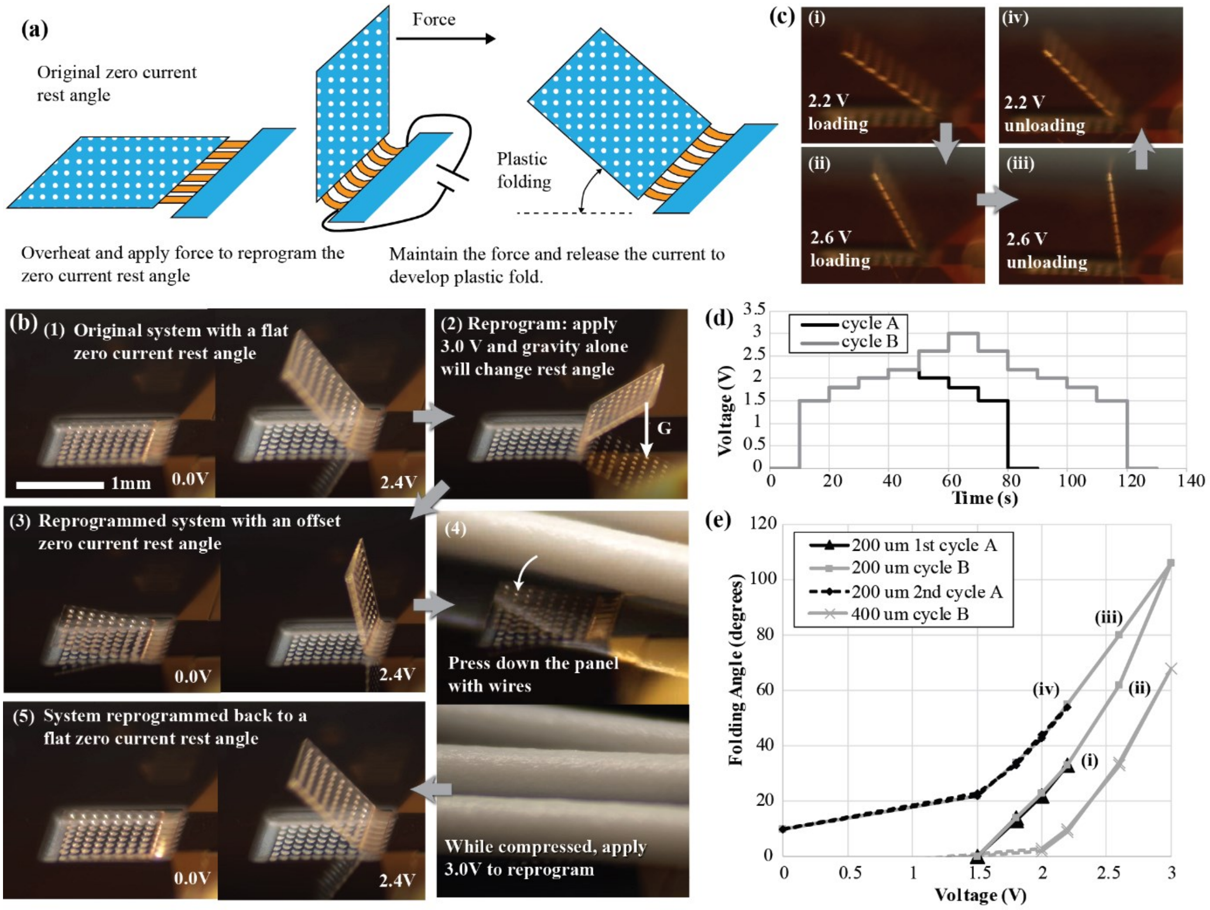

Figure 3. Plastic folding behavior of the micro-origami. (a) A schematic illustration of achieving the plastic folding by reprograming the zero current rest angle of creases. (b) An experimental test that twice reprograms the zero current rest angle of a single-crease origami system with 200 µm long actuator (see Video S2). (c) Pictures of the hysteretic folding behavior of a single-crease origami with 200 µm beams under the loading cycle B; (d) Loading cycles used for measuring the hysteretic elasto-plastic behavior; (e) Hysteretic voltage-angle curves for the single-crease origami.

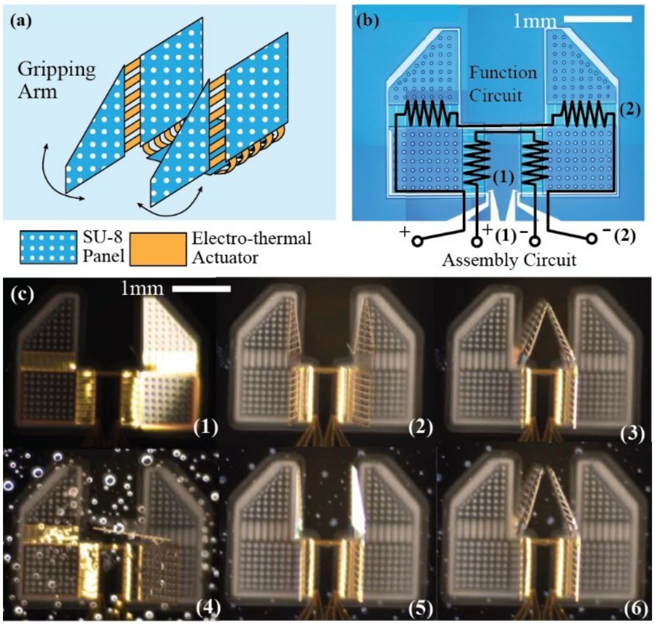

Figure 4. A large motion range origami gripper. (a) A 3D illustration of the reconfigurable gripper that can self-assemble; (b) A microscope picture of the 3D reconfigurable gripper before release with an illustration of the circuit design. Circuit (1) connects the two arrays for assembling the 3D gripper while circuit (2) connects the two gripper arrays; (c) The assembling and gripping motion of the 3D gripper. This functional 3D gripper can survive a wet environment and remains functional after drying. (See Video S3)

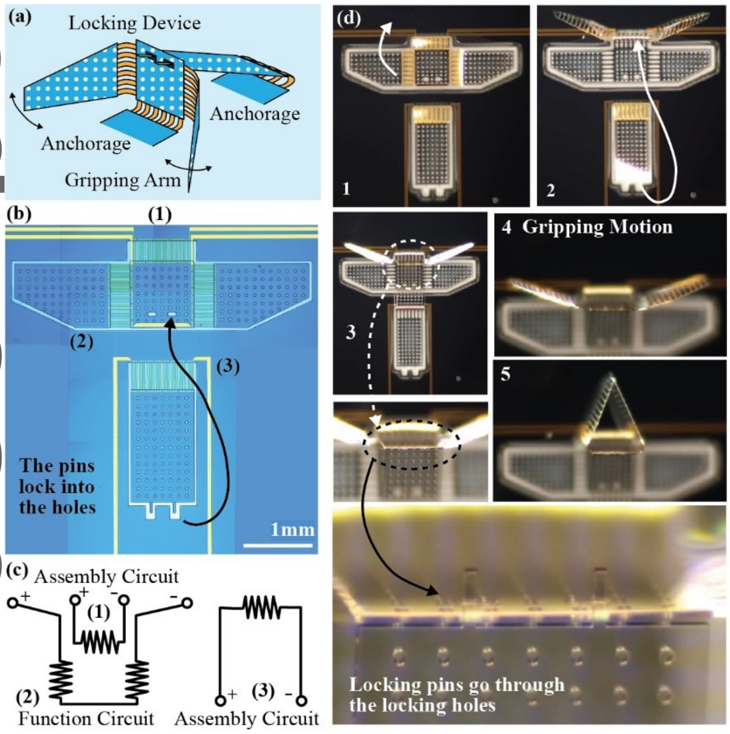

Figure 5. Locking origami gripper. (a) A 3D illustration of a reconfigurable gripper that can lock itself in a folded configuration; (b) Microscope image of the system; (c) An illustration of the circuit design. Circuits (1) and (3) facilitate assembly of the structure, while circuit (2) is used for the gripper actuation; (d) The assembly and gripping process include: aligning the locking pins to the holes, locking the 3D configuration, and actuating the gripping arms. The bottom picture is a close-up of the locking devices, with which the gripper can holds the 3D configuration without continuous input of energy. (See Video S4)

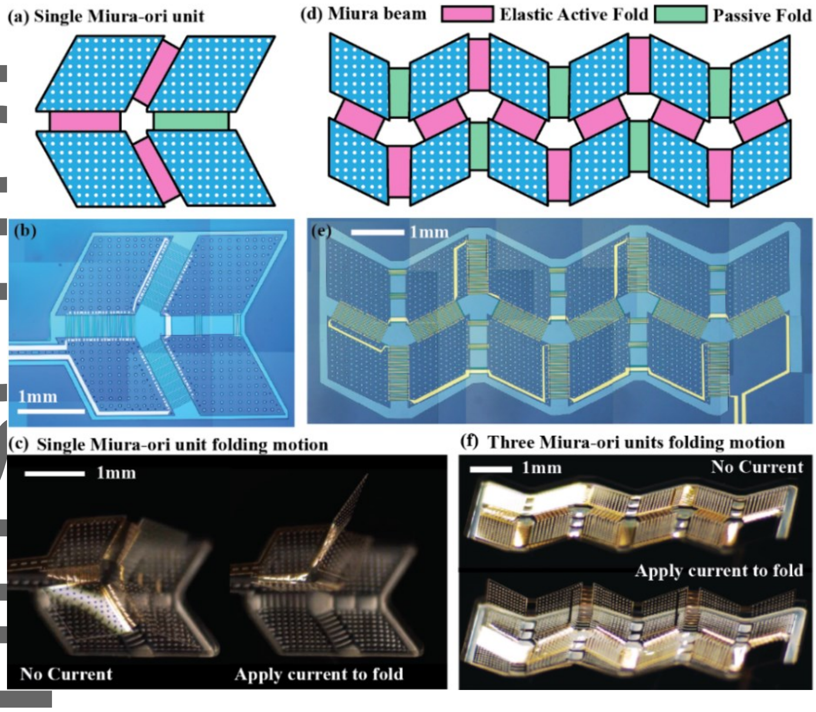

Figure 6. Combining elastic active folds and passive folds for origami with both mountain and valley folds: (a) Design of active and passive folds for the single Miura-ori pattern; (b) A microscope picture of a single Miura-ori unit with three active folds and a passive fold before release; (c) The folding motion of this single Miura-ori unit; (d) Design of active and passive folds for the three unit Miura-ori pattern; (e) A microscope picture of a three unit Miura-ori with active and passive folds before release; (f) The folding motion of the three unit Miura-ori. (Video S5)

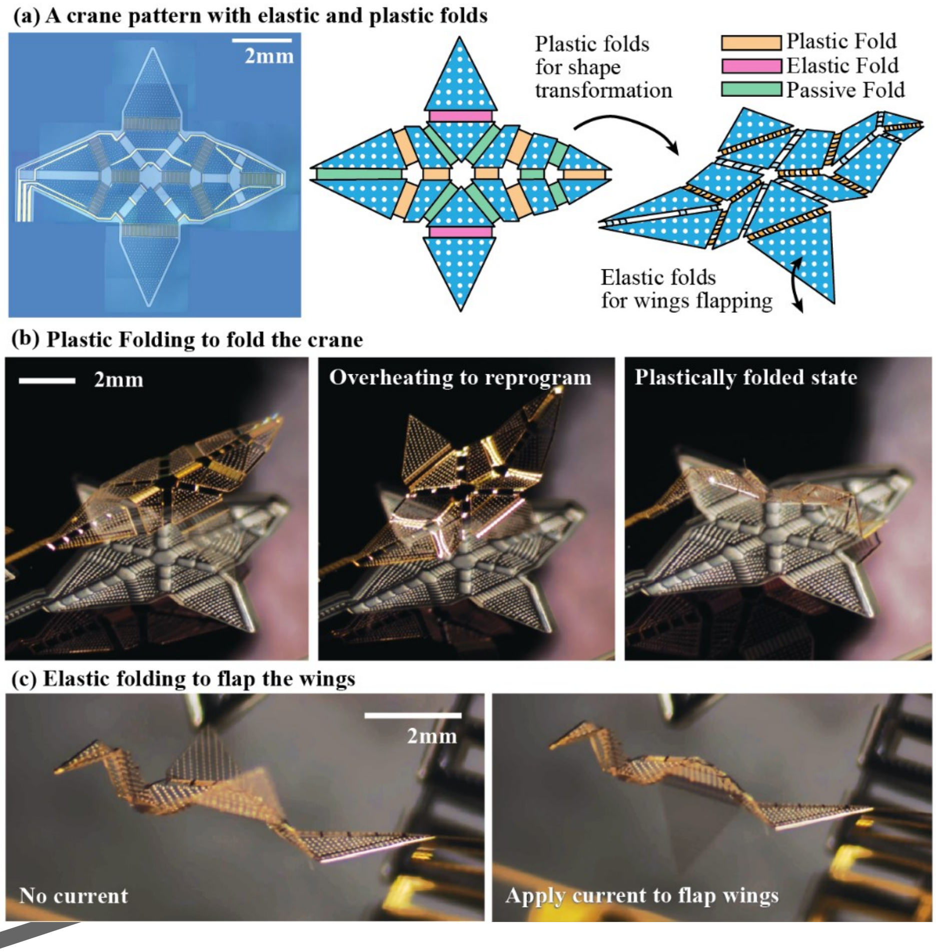

Figure 7. Combining elastic and plastic folding enables functional complex origami systems. (a) A microscope picture and an illustration of the origami crane pattern that can achieve plastic shape transformation and can flap its wings elastically; (b) Plastically folding the crane pattern by overheating the creases to reprogram their zero current rest angle; (c) The elastic folding is used to flap the wings of the crane pattern. (Video S5)

An elastically and plastically foldable micro-origami is developed and tested to create controllable and functional 3D shape morphing systems with multiple active degrees-of-freedom. The work demonstrates a versatile design-fabrication-actuation method to achieve rapid folding, enhanced control, and function in different atmospheric environments, enabling applications in micro-robots, medical devices, and metamaterials.

Keyword: Micro-Origami

*Yi Zhu, Mayur Birla, Kenn Oldham, and Evgueni T. Filipov**

Elastically and Plastically Foldable Electro-Thermal Micro-Origami for Controllable and Rapid Shape Morphing